Preparation of Visible-light Responsive Rutile-TiO2 (110) Wafer with Well-defined Surface by Chromium and Antimony Codoping

Kitta, Mitsunori

Onishi, Hiroshi

(Citation)
e-Journal of Surface Science and Nanotechnology,17:5-9

(Issue Date)
2019-02-14

(Resource Type)
journal article

(Version)
Version of Record

(URL)
https://hdl.handle.net/20.500.14094/90005641

eJSSNT Regular Paper

e-Journal of Surface Science and Nanotechnology **17**, 5−9 (2019)

Preparation of Visible-light Responsive Rutile-TiO_2 (110) Wafer with Well-defined Surface by Chromium and Antimony Codoping

Mitsunori Kitta,[†, ‡] Hiroshi Onishi

Department of Chemistry, Kobe University, Rokkodai, Nada, Kobe, 657-8501, Japan
[†] *Present address: Research Institute of Electrochemical Energy, Department of Energy and Environment, National Institute of Advanced Industrial Science and Technology (AIST), 1-8-31, Midorigaoka, Ikeda, Osaka, 563-8577, Japan*
[‡] *Corresponding author: m-kitta@aist.go.jp*

Received: 28 December, 2018; Accepted: 1 February, 2019; Published: 14 February, 2019

Transition-metal doping for titanium dioxide (TiO_2) is attracting attention for the study of visible-light responsive photocatalyst. Its photocatalytic properties were investigated via various spectroscopic approaches, though surface studies had not yet progressed owing to the difficulty in obtaining its well-defined surface. In this report, we propose that a well-defined crystalline TiO_2(110) surface may be obtained by the codoping of chromium (Cr) and antimony (Sb) with commercially available wafers. Cr and Sb are codoped by a solid-state reaction of TiO_2(110) wafer and dopant powder. The prepared wafer exhibited visible-light responsivity on absorption below wavelengths of 600 nm. The surface morphology characterization, performed by atomic force microscopy (AFM) revealed that the Cr and Sb codoped TiO_2(110) surface has a well crystallized step-terrace structure that is atomically flat, while monodoped TiO_2(110) surface does not. The codoping of Cr and Sb with TiO_2(110) wafer should contributes towards retaining the stable rutile-TiO_2 lattice structure and produces a well-defined TiO_2(110) surface structure with visible-light responsive characteristics.

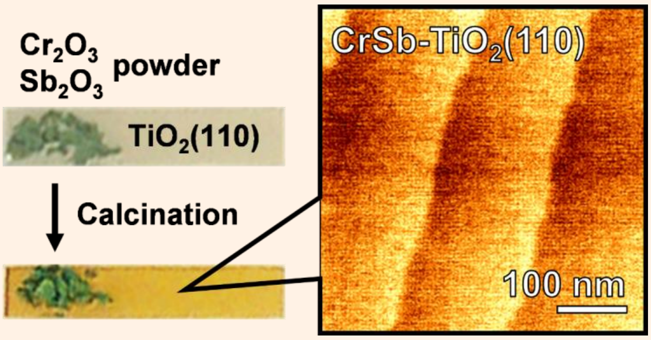

Keywords *Visible-light responsive photocatalyst; Doped rutile-TiO_2; Cr and Sb codoping; Well-defined surface; Atomic force microscopy*

I. INTRODUCTION

Titanium dioxide doped with certain transition metals exhibit attractive properties and potentialities for making functional materials such as gas sensors [1], catalysts [2−4], electrodes [5], and fine ceramics [6]. Especially, it has been discovered that doping transition metals into titanium dioxides increases the visible-light absorption, and this is promising in manufacturing practical photocatalysts that operate under sun-light irradiation. Therefore, titanium dioxides doped with transition metals have been extensively investigated via various viewpoints such as spectroscopic study [7] and calculating approach [8].

Conventionally, sol-gel, wet impregnation, hydrothermal synthesis, etc. were widely used for introducing transition metals into TiO_2 and the doped materials prepared by these methods were investigated as visible-light responsive photocatalysts. However, as the materials that are prepared using conventional doping methods are mostly powders or have polycrystalline forms, it became difficult to perform fine surface studies. As the photocatalytic reaction is triggered in the bulk phase as well as on the surface, the surface observation of the transition metal doped TiO_2 is important for photocatalytic studies. It will provide us with considerable information for elucidating photocatalyst properties, such as the surface structure [9], desorption and adsorption mechanism of reactants [10, 11], etc. Therefore, it is highly desirable to employ doped TiO_2 wafer surfaces with well-defined structures to perform scientific surface research.

To address this issue, we proposed the codoping of chromium (Cr) and antimony (Sb) with $TiO_2(110)$ wafer as a promising alternative for acquiring a well-defined $TiO_2(110)$ surface with visible-light response. We used commercial rutile-$TiO_2(110)$ wafer and prepared monodoped $TiO_2(110)$ wafer with Cr or Sb, and further codoped $TiO_2(110)$ wafer samples via a solid-state reaction, which was conventionally used for making ceramic powder and several doping materials that exhibit high photocatalytic activities are produced via this method [12, 13]. Note that rutile TiO_2 codoped with Cr and Sb functions as a visible-light responsive photocatalyst [14] and its photocatalytic properties have been widely investigated [14–16]. The prepared doped samples were assessed using optical absorption and contact-mode atomic force microscopy (AFM) imaging to reveal the dependency of the preparing conditions on their surface structure.

II. EXPERIMENTAL SECTION

Rutile $TiO_2(110)$ wafer, purchased from SHINKOHSHA, Co. Ltd., cut into 10 mm × 2 mm × 0.5 mm sized samples were codoped with Cr and Sb via conventional solid-state reactions. The dopant materials, Sb_2O_3 and Cr_2O_3 powders, (99.9%, purchased from Wako-chemical, co. Ltd.) were mixed in a molar ratio of 1 : 1, and placed on the polished surface of the $TiO_2(110)$ wafer. Next, calcination at 1270 K in air for 22 h using alumina crucibles (99.7% Al_2O_3) was performed. The Al_2O_3 crucible was sealed to prevent escape of evaporated Sb oxide. During the calcination process, the dopant diffuses with the wafer surface. The detailed procedure of the sample preparation is shown in Figure S1 (Supplementary Material). After calcination, $TiO_2(110)$ wafer turns from white to yellow in color, indicating the acquired visible-light absorption property, which was further confirmed via UV-VIS diffuse reflection spectroscopy. To measure the spectra, we used integrating-sphere measurement, and the doped wafers were attached to the sample holder with their polished surfaces upwards. Surface observation was performed by scanning probe microscopy (JSPM-4200, JEOL. Inc.) along with contact-mode AFM in air at room temperature.

III. RESULTS AND DISCUSSION

Figure 1(a) shows photographs of various sample wafers. The sample before calcination (upper column) exhibited white color as pristine $TiO_2(110)$ wafer (a non-doped sample), while the sample prepared with pure Cr_2O_3 powder (middle column) exhibited dark color. In the powder characterization, the monodoping of Cr_2O_3 (Cr^{3+}) with TiO_2 generate oxygen vacancies or the higher oxide state of chromium cations (Cr^{6+}), owing to the compensation of charge neutralities of Cr^{3+} and Ti^{4+} substitution. Therefore, monodoped TiO_2 (Cr-TiO_2) has various impurity states in the bandgap of TiO_2, leading to the absorption of photons with various energies, and the color turns from white to black [14]. The features of the prepared Cr-$TiO_2(110)$ wafer sample corresponded well corresponding with these findings. On the other hand, $TiO_2(110)$ wafer codoped with Cr/Sb ($Cr_2O_3 : Sb_2O_3 = 1 : 1$ mixed) powder, as shown in the lower column showed clear yellow color. The codoping of Cr and Sb into the TiO_2 lattice, where Cr^{3+} and Sb^{5+} were substituted with $2Ti^{4+}$ maintained the charge neutrality. No oxygen vacancies were generated, and doped chromium had a fixed oxide state as Cr^{3+}. Therefore, the codoped TiO_2 has yellow color as its photon absorption is exactly derived from the fixed $Cr^{3+} \rightarrow Ti^{4+}$ charge transfer [14]. Figure 1(b) shows the UV-VIS diffuse reflection spectra of the doped $TiO_2(110)$ wafers. Codoped TiO_2 sample displayed absorption bands due to the $Cr^{3+} \rightarrow Ti^{4+}$ charge transfer transition in the visible-light region ($\lambda < 600$ nm) in contrast to pristine

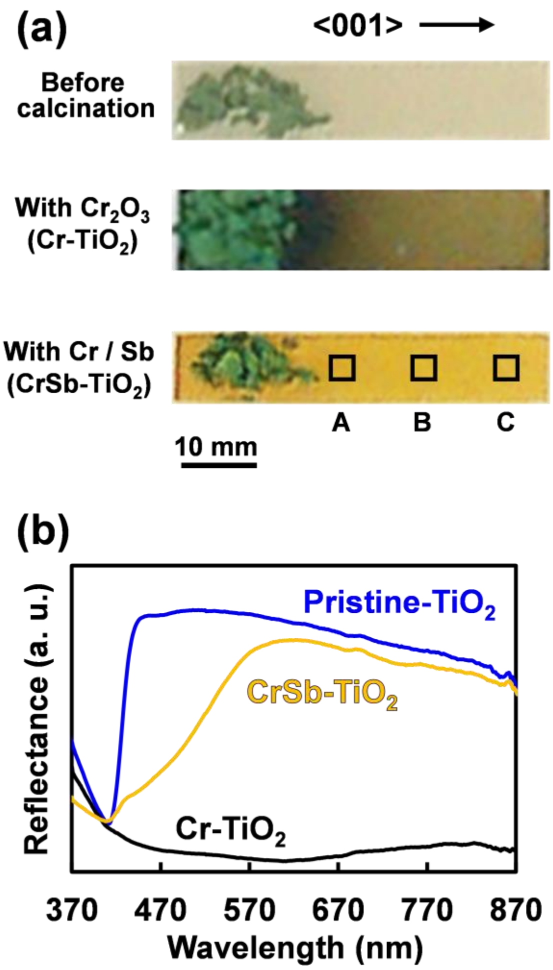

Figure 1: Prepared samples and their photo-absorbed properties. (a) Photographs of the $TiO_2(110)$ wafer samples before calcination (upper), monodoped with Cr (middle), and codoped with Cr and Sb (lower). The AFM scanning positions corresponding to Figure 3 are indicated on the photograph of CrSb-$TiO_2(110)$ wafer by the black square areas. (b) Diffuse reflection spectra of the prepared samples. The (110) wafers of non-doped TiO_2, Cr-TiO_2, and CrSb-TiO_2 are represented by blue, black, and yellow solid lines, respectively.

$\mathrm{TiO_2}$. Monodoped $\mathrm{TiO_2}$ with only Cr (Cr-$\mathrm{TiO_2}$) displayed wide absorption in the visible-light region as reported in the previous study pertaining to powders [14]. From these results, it is apparent that we would prepare visible-light responsive $\mathrm{TiO_2}$(110) wafers with transition metal doping.

In the doped $\mathrm{TiO_2}$(110) wafers, the polished specular surface was retained except in the lower region of the powder, and it allowed us to acquire meaningful AFM images on their surfaces. Figure 2 presents the contact-mode AFM images of doped $\mathrm{TiO_2}$(110) wafers. Figure 2(a) shows the surface structure of pristine $\mathrm{TiO_2}$(110) treated with the same calcination conditions of doped wafer (heated 1270 K in air for 22 h) without the dopant powder. One can observe some terraces, and the step structure is dominated by step edges running parallel to the $\langle 001 \rangle$ direction [9], similar to the typical well-defined structure of the non-doped $\mathrm{TiO_2}$(110) surface. In contrast, the surface of the Cr doped wafer as shown in Figure 2(b) is not similar to the well-defined $\mathrm{TiO_2}$(110) surface structure. As explained above, when $\mathrm{Cr^{3+}}$ ions are partly substituted for $\mathrm{Ti^{4+}}$ ions in $\mathrm{TiO_2}$, oxygen vacancies and/or $\mathrm{Cr^{6+}}$ ions should be formed to keep the charge balance, and they may cause the disarrangement of the rutile structure [14]. These structural deteriorations of the Cr-$\mathrm{TiO_2}$(110) surface were observed at any part and on various imaging scales, as shown in Figure S2 (Supplementary Material).

Figure 2(c) shows the surface structure of wafer that is doped with only Sb. Several streaky structures that extend in the $\langle 001 \rangle$ direction were observed. When only Sb is doped with $\mathrm{TiO_2}$, $\mathrm{Sb^{3+}}$ and $\mathrm{Sb^{5+}}$ were produced to maintain the charge neutrality, and they formed double oxides ($\mathrm{Sb^{3+}Sb^{5+}O_4}$) [17]. We assume that the streaky structures are made by these double oxides extending along the $\langle 001 \rangle$ direction of the rutile $\mathrm{TiO_2}$(110) surface. On the other hand, as shown in Figure 2(d), the result of the $\mathrm{TiO_2}$(110) wafer codoped with Cr and Sb is different from any case of the monodoped $\mathrm{TiO_2}$(110) wafer surface. The surface resembles the pristine $\mathrm{TiO_2}$(110) well-defined structure. Figure 2(e) shows the surface profile along with the A−B line of Figure 2(d). The step height is approximately 0.3 nm and this is well in agreement with the height of the single step of the (110) surface of the rutile $\mathrm{TiO_2}$. These results indicate that the $\mathrm{TiO_2}$(110) wafer codoped with Cr and Sb resembles the rutile type structure, and the reason behind this may be explained in terms of crystallography. When Cr and Sb are codoped with $\mathrm{TiO_2}$, it is known that $\mathrm{Cr^{3+}}$ and $\mathrm{Sb^{5+}}$ produce a double oxide ($\mathrm{CrSbO_4}$). Furthermore, $\mathrm{CrSbO_4}$ resembles the rutile type structure ($a = b = 4.59$ Å, $c = 3.05$ Å) similar to the $\mathrm{TiO_2}$ crystal ($a = b = 4.59$ Å, c = 2.953 Å) [18]. Eventually, Cr and Sb were codoped without disturbing the $\mathrm{TiO_2}$ rutile structure.

It is known that the photocatalytic activities of $\mathrm{TiO_2}$ codoped with Cr and Sb are remarkably increased in comparison with only Cr doped $\mathrm{TiO_2}$ [14] and the reason for this is explained in terms of photo-induced dynamics. However, photocatalytic activities of doped $\mathrm{TiO_2}$ are controlled by not only the photo-dynamic processes in bulk, but by the condition of their surface structures as well, as the catalyst reaction occurs on the crystal surface, and our result reflects this point. The surface of the codoped $\mathrm{TiO_2}$(110) wafer is considerably more crystallized than that of the only Cr doped $\mathrm{TiO_2}$, and we suggest that the differences in their surface structures is influenced by the differences in their catalytic activities.

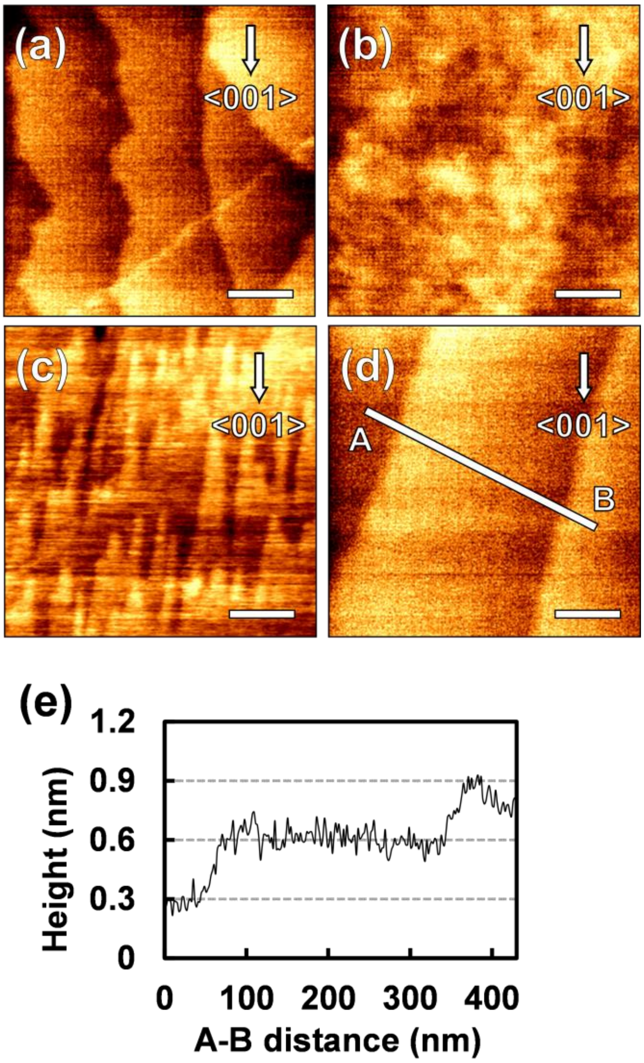

Figure 2: Contact-mode AFM images of the doped $\mathrm{TiO_2}$(110) wafer surface. (a) Pristine $\mathrm{TiO_2}$, (b) $\mathrm{TiO_2}$ doped with only Cr, (c) $\mathrm{TiO_2}$ doped with only Sb, and (d) $\mathrm{TiO_2}$ codoped with both Cr and Sb. The entire scale bar is 100 nm long. (e) Topographic profile along with the A−B line as shown in (d).

We prepared $\mathrm{TiO_2}$(110) wafer samples codoped with Cr and Sb under various calcination times (for 12 h, 22 h, and 30 h). AFM images of prepared sample surfaces were summarized in Figure 3. In these samples, the surface observation was performed on three parts of the wafer surface as shown in A−C of Figure 1(a). In the prepared sample calcinations for 12 h, we can observe some steps and terraces on the surface at position A. This structure resembles the surface structure of codoped $\mathrm{TiO_2}$(110) wafer as in Figure 2(d).

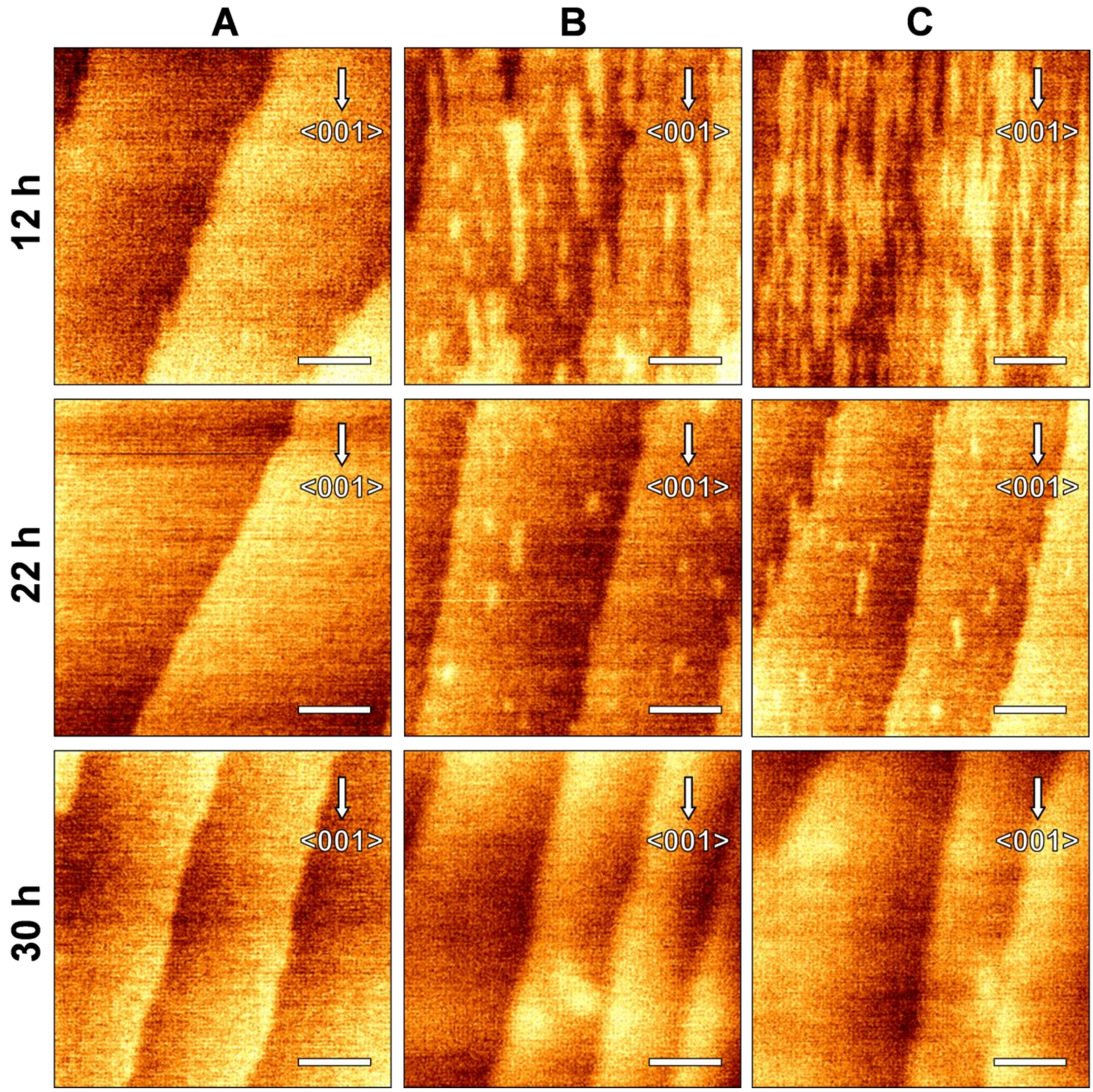

Figure 3: Contact-mode AFM images of CrSb-TiO_2(110) wafer prepared with various calcination times. Upper, middle, and lower lines correspond to the calcination times of 12 h, 22 h, and 30 h, respectively. Each column from A to C displays the observing positions corresponding to the positions A, B, and C in Figure 1(a). The entire scale bar is 100 nm long.

Although the same sample, several streaky structures were observed at position C and this surface structure is similar to that observed on the wafer only doped with Sb as shown in Figure 2(c). These characteristic surface structures were further observed at various imaging scales, as shown in Figure S3 (Supplementary Material). From this, we estimate that Sb was excessively doped compared to Cr at the far position from dopant powder source, and it is indicated that Sb diffuses more quickly than Cr in spite of its atomic weight. This can be explained by the volatilization of Sb oxide. During the calcination process, a part of the Sb oxide will be volatilizing, and spreading on the wafer surface as vapor phase. Note that the vaporized Sb-oxide should fill the sealed Al_2O_3 crucible. Therefore, the Sb dopant is contacted with the TiO_2 wafer surface to a greater extent than the Cr dopant and will be quickly doped on any part of the TiO_2 wafer surface via vapor-solid interface reaction. Once the Sb was doped into TiO_2 lattice, formed Sb-TiO_2 should be stable and Sb would not evaporate from the rutile lattice.

At the same observation position, the surface structures vary with respect to the calcination times. Step and terrace structures of the rutile (110) are more reproduced by longer calcinations times. When the sample is calcined for 30 h, its surface structure is uniform at any observation position as the Cr dopant is diffused adequately to reconstruct the rutile structure. Eventually, the surface structure of the codoped TiO_2(110) wafer depends on the diffusing process of Cr, and a longer calcinations time allows us to prepare the well codoped TiO_2(110) surface with a clear step and terrace structure. It should be suitable for basic surface studies, will aid in reaching fine atomic scale investigations [19].

IV. CONCLUSIONS

We prepared a visible-light responsive TiO_2(110) wafer with a well-defined surface structure along with an atomically flat step and terrace, via the codoping of Cr and Sb through a conventional solid-state reaction. The prepared TiO_2(110) wafer codoped with Cr and Sb exhibited visible-light absorption that arises from the $Cr^{3+} \rightarrow Ti^{4+}$ charge transfer transition. The prepared doped TiO_2(110) wafer retains its polished specular surface except for the region beneath the dopant powder and was appropriate for AFM imaging. The surface structure of the monodoped Cr-TiO_2(110) wafer was clearly varied from the pristine TiO_2(110) surface. However, the surface structure of rutile TiO_2(110) is maintained by codoping with Cr and Sb. We estimated that the diffusion of the Cr dopant is rate-determining during the codoping process owing to the volatility of the Sb oxides. We prepared CrSb-TiO_2(110) wafer with a well-defined step and terrace surface structure via adequate codoping. The wafer will be suitable for the basic surface study of visible-light responsive photocatalysts.

Appendix

A detailed procedure of sample preparation and various AFM images of Cr-TiO_2(110) and CrSb-TiO_2(110) are available in Supplementary Material at https://doi.org/10.1380/ejssnt.2019.5.

References

[1] A. M. Ruiz, G. Sakai, A. Cornet, K. Shimanoe, J. R. Morantea, and N. Yamazoe, Sens. Actuators B **93**, 509 (2003).
[2] K. T. Ranjit and B. Viswanathan, J. Photochem. Photobiol. A **108**, 79 (1997).
[3] S. Klosek and D. Raftery, J. Phys. Chem. B **105**, 2815 (2001).
[4] R. Q. Long and R. T. Yang, Appl. Catal. B **24**, 13 (2000).
[5] Y. Wang, H. Cheng, Y. Hao, J. Ma, W. Li, and S. Cai, Thin Solid Films **349**, 120 (1999).
[6] V. C. Sousa, E. R. Leite, J. A. Varela, and E. Longo, J. Eur. Ceram. Soc. **22**, 1277 (2002).
[7] W. Choi, A. Termin, and M. R. Hoffmann, J. Phys. Chem. **98**, 13669 (1994).
[8] T. Umebayashi, T. Yamaki, H. Itoh, and K. Asai, J. Phys. Chem. Solids **63**, 1909 (2002).
[9] U. Diebold, Surf. Sci. Rep. **48**, 53. (2003).
[10] H. Onishi, Y. Yamaguchi, K. Fukui, and Y. Iwasawa, J. Phys. Chem. **100**, 9582 (1996).
[11] M. Aizawa, Y. Morikawa, Y. Namai, H. Morikawa, and Y. Iwasawa, J. Phys. Chem. B **109**, 18831 (2005).
[12] H. Kato, K. Asakura, and A. Kudo, J. Am. Chem. Soc. **125**, 3082 (2003).
[13] A. Kudo, K. Ueda, H. Kato, and I. Mikami, Catal. Lett. **53**, 229 (1998).
[14] H. Kato and A. Kudo, J. Phys. Chem. B **106**, 5029 (2002).
[15] T. Ikeda, T. Nomoto, K. Eda, Y. Mizutani, H. Kato, A. Kudo, and H. Onishi, J. Phys. Chem. C **112**, 1167 (2008).
[16] C. Di Valentin, G. Pacchioni, H. Onishi, and A. Kudo, Chem. Phys. Lett. **469**, 166 (2009).
[17] G. Ren, C. Wang, J. Xia, J. Liu, and H. Zhong, Mater. Lett. **63**, 605 (2009).
[18] J. Amador and I. Rasines, J. Appl. Cryst. **14**, 348 (1981).
[19] R. Bechstein, M. Kitta, J. Schütte, A. Kühnle, and H. Onishi, J. Phys. Chem. C **113**, 13199 (2009).

Published by The Japan Society of Vacuum and Surface Science